sustainability

MDPI

Article

The Effect of Electricity Generation on the Performance of Microbial Fuel Cells for Anammox

Wenqin Jiang [1], Jian Zhang [2], Qiulin Yang [2] and Ping Yang [1,*]

[1] College of Architecture and Environment, Sichuan University, Chengdu 610207, China; 13060026309@163.com
[2] Sichuan Development Environmental Science and Technology Research Institute Co., Ltd., Chengdu 610041, China; zhangjian8397@163.com (J.Z.); yangqiulin1111@163.com (Q.Y.)
* Correspondence: yangpinga301@163.com; Tel./Fax: +86-28-61916262

Abstract: The Anammox anaerobic fluidized bed microbial fuel cell (Anammox AFB-MFC) exhibits exceptional performance in both nitrogen removal and electricity generation, effectively eliminating ammonia nitrogen (NH_4^+-N) and nitrite nitrogen (NO_2^--N) pollutants. This technology offers the advantages of high efficiency in nitrogen removal and low electricity consumption. By coupling an AFB with an MFC, the Anammox AFB-MFC was developed through the introduction of anaerobic ammonia-oxidizing bacteria (AnAOB) into MFC. Anammox AFB-MFC's nitrogen removal ability was found to be superior at an influent COD concentration of 200 mg/L, as determined by a study conducted under unchanged conditions. Subsequently, an open and closed-circuit experiment was performed on the Anammox AFB-MFC system while maintaining a COD concentration of 200 mg/L in the influent. Remarkably, the reactor exhibited significantly enhanced nitrogen removal performance when electricity generation occurred. Throughout the entire experimental process, the reactor consistently maintained high nitrogen removal efficiency and electricity production performance. Under optimal experimental conditions, the reactor achieved a remarkable nitrogen removal rate of 91.8% and an impressive output voltage of 439.1 mV. Additionally, the generation of Anammox bioparticles in MFC significantly contributed to efficient pollutant removal. This study elucidates the impact of organic matter on both the nitrogen removal and electricity generation capabilities of Anammox AFB-MFC, as well as highlights the synergistic effect between MFC electricity generation and nitrogen removal in the reactor.

Keywords: anaerobic ammonia oxidation; microbial fuel cells; anaerobic fluidized bed; electricity generation; Anammox bioparticles

Citation: Jiang, W.; Zhang, J.; Yang, Q.; Yang, P. The Effect of Electricity Generation on the Performance of Microbial Fuel Cells for Anammox. *Sustainability* **2024**, *16*, 2705. https://doi.org/10.3390/su16072705

Academic Editor: Paolo S. Calabrò

Received: 9 February 2024
Revised: 17 March 2024
Accepted: 21 March 2024
Published: 25 March 2024

1. Introduction

In recent years, the presence of nitrogen-containing pollutants in water has exerted a significant impact on the aquatic environment, making them the primary contributors to water pollution [1,2]. Biological nitrogen removal technology has gained significant attention due to its economic efficiency and mild operating conditions compared to physical and chemical methods for nitrogen removal. Extensive research has been conducted on the existing biological nitrogen removal technology for treating wastewater with low-concentration nitrogen and a high C/N ratio. However, the challenge lies in achieving efficient nitrogen removal from wastewater with a high concentration nitrogen and a low carbon-to-nitrogen ratio, which is crucial for effective water pollution control [3]. The anaerobic ammonia oxidation (Anammox) process is a cost-effective and highly efficient biological nitrogen removal technology utilized in wastewater treatment. It involves the anaerobic conversion of nitrite (NO_2^--N) into nitrogen gas (N_2) by specialized bacteria known as anaerobic ammonia oxidation bacteria (AnAOB), which utilize ammonia nitrogen (NH_4^+-N) as an electron donor under anaerobic or anoxic conditions (Figure 1). Compared to conventional biological nitrogen removal processes, the Anammox technology offers several advantages,

such as reduced energy consumption for aeration, decreased organic carbon requirements, minimized sludge production, and improved economic viability. This emerging sewage nitrogen removal solution holds significant potential for replacing traditional nitrogen removal methods [4]. To date, a total of five genera of AnAOB have been identified, namely *Candidatus Brocadia*, *Candidatus Kuenenia*, *Candidatus Jettenia*, *Candidatus Scalindua*, and *Candidatus Anammoxoglobus* [5]. Bioelectrochemical systems (BES) combine electrochemical and biological methods, improving the drawbacks of biological methods such as a long start-up time, a low nitrogen removal rate, and the need for additional carbon sources. They also solve the problem of high energy consumption in electrochemical methods. Meanwhile, BES can generate electricity while achieving wastewater nitrogen removal treatment, reducing sludge production, and having advantages that traditional processes cannot match. It is an effective and economical nitrogen removal method. In recent years, the use of bioelectrochemical processes to treat nitrogen-containing wastewater has become a research hotspot [6]. Among all BESs, the microbial fuel cell (MFC) has obvious advantages and is widely studied [7]. MFC is a device that employs electrogenic microorganisms to catalyze the oxidation of pollutants in wastewater, thereby directly converting the chemical energy stored in the pollutants into electrical energy [8]. The commonly employed dual-chamber MFC comprises three components: an anode chamber, a cathode chamber, and a proton exchange membrane (PEM). The PEM serves the purpose of segregating the two electrode chambers while facilitating the transport of protons within the electrode chamber. Each of the two chambers contains an electrode, namely the anode and cathode, through which electrons traverse in the external circuit [9]. The electrochemical process of MFCs can be described as follows: Within the anode chamber, electricity-generating microorganisms proliferate and metabolize organic matter present in wastewater, thereby undergoing oxidation reactions that result in electron and proton release. Initially, electrons are transferred from intracellular electron transfer chains to microbial cell membranes before being conveyed to the anode via electron transfer mechanisms. Subsequently, these electrons are transmitted from the anode to the cathode through an external circuit, where they engage in reduction reactions with protons traversing through the PEM within the cathode chamber [10]. The utilization of MFCs for nitrogen removal in wastewater can be achieved under conditions with lower carbon-to-nitrogen ratios (C/N). Additionally, MFCs provide several advantages, including a diverse range of fuel sources, operation in mild conditions, less sludge production [11], high energy conversion efficiency, large volume load capacity, and environmental friendliness [4]. The integration of MFC with other sewage treatment technologies facilitates the simultaneous removal of pollutants and the generation of electricity.

The electric field generated by MFC can enhance the activity of Anammox bacteria responsible for nitrogen removal. Moreover, the MFCs can utilize NH_4^+-N in the Anammox system as a fuel source, while their output voltage serves as an external power supply for the Anammox process [12]. Additionally, this coupled system facilitates various processes, including ammonia oxidation, Anammox, nitrification, and denitrification. Consequently, this integrated approach enables simultaneous removal of NH_4^+-N and NO_2^--N from wastewater while generating electricity and minimizing carbon source addition and energy consumption. This renders it an economically efficient nitrogen removal process. The Anammox MFC integrates two energy-efficient technologies for wastewater treatment, thereby facilitating efficient nitrogen removal and enabling energy recovery. In recent years, the integration of MFC with Anammox has been investigated, and its performance has been evaluated through comprehensive testing and analysis.

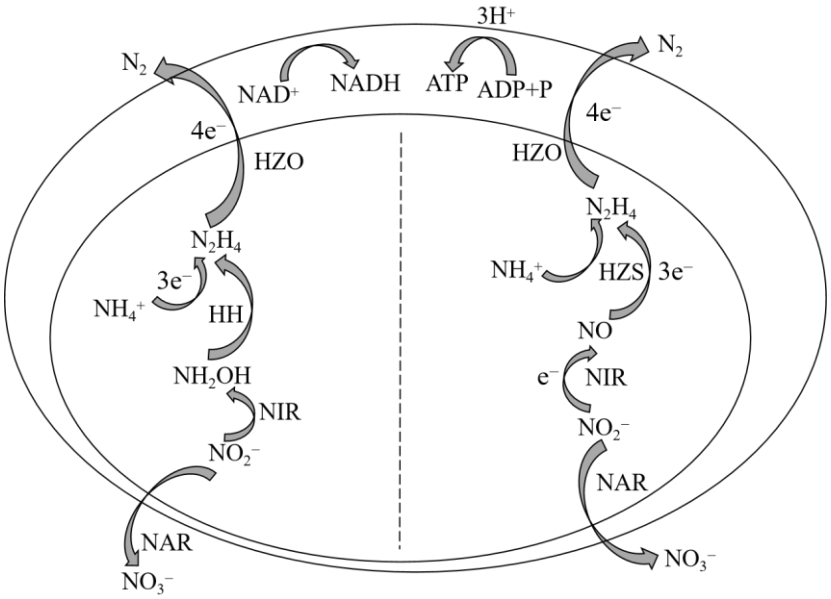

Figure 1. Metabolic pathways of anammox reaction.

Both the anode and cathode chambers of the Anammox MFC can undergo nitrogen removal processes. Based on the inoculation method of Anammox sludge and the configuration of the MFC reactor, it can be categorized into anode inoculation and cathode inoculation. Anodic inoculation refers to the introduction of activated sludge containing AnAOB into the anode chamber of MFC, where a consortium of denitrifying bacteria (DNB), AnAOB, and electricity-producing bacteria coexist. The inoculation of Anammox sludge into the anode chamber of MFC resulted in a remarkable total nitrogen removal rate exceeding 80% and an impressive output power density (PA) ranging from 1.26 to 1.35 W/m^3 [13]. Cathodic inoculation refers to the inoculation of activated sludge containing AnAOB in the cathode chamber of MFC. In the anode chamber, organic substances such as glucose and sodium acetate are used as anode substrates, and electrons are transferred from the anode to the cathode through an external circuit. The autotrophic DNB in the cathode receives electrons, reduces NO_2^--N and NO_3^--N, and simultaneously undergoes autotrophic nitrogen removal reactions, converting nitrate and nitrite into nitrogen to achieve nitrogen removal. Li et al. inoculated sludge containing AnAOB in the MFC cathode chamber, and the results showed that this cathode inoculation can promote the removal of NH_4^+-N and NO_2^--N [14]. Xu et al. [15] successfully constructed a high nitrogen-loaded dual-chamber MFC coupled with the Anammox reaction and demonstrated their stable initiation and operation at NH_4^+-N concentrations of 400 mg/L and NO_2^--N concentrations of 528 mg/L.

The performance of Anammox MFC is influenced by various factors, including temperature, HRT, DO, and pH, which are crucial parameters affecting the performance of the coupled system. Notably, low temperatures significantly inhibit the activity of AnAOB. Previous studies have demonstrated that Anammox is less efficient at 15 °C compared to 30 °C [16]. If the HRT is too long, Anammox will experience prolonged starvation, which can negatively impact both the nitrogen removal rate and electricity production performance. Conversely, if HRT is too short, it may reduce the nitrogen removal rate. Additionally, since Anammox is an anaerobic bacterium, dissolved oxygen levels in the reactor can significantly affect its activity and thus influence Anammox. The effect of DO concentration on the nitrogen removal and carbon removal performance of MFC was investigated by YU et al. [17]. It was found that under low DO concentration conditions (0.5 mg/L), the nitrogen removal efficiency of MFCs was twice as high compared to high DO concentration conditions (2 mg/L), while the COD removal rate did not exhibit significant changes. These results suggest that a lower DO concentration is advantageous for the

nitrogen removal process in MFCs. The enzyme activity of DNB and electrogenic bacteria is significantly influenced by the pH value. Previous studies have demonstrated that the Anammox reaction rate reaches its maximum at a pH value of 8, resulting in a nitrogen removal rate of 1.42 kg/(m^3·d) [18]. However, there has been limited investigation into the power generation performance of the MFC coupling system and its impact on reactor nitrogen removal performance.

In contrast to conventional Anammox nitrogen removal technology, the Anammox–MFC coupling system enables simultaneous electricity generation and nitrogen removal, with the potential for enhanced nitrogen removal through electric field stimulation. Currently, there is a lack of comprehensive understanding regarding the nitrogen removal mechanism in the Anammox–MFC coupling system and the underlying principles behind electric field enhancement during MFC-mediated nitrogen removal. Therefore, it is imperative to thoroughly investigate its operational mechanisms.

To comprehensively understand the impact of MFC power generation on Anammox–MFC performance, we investigated the NRE and power generation efficiency of the system under various operating conditions. Different from SBR and UASB reactors, the distinctive advantage of AFB in this experiment lies in its utilization of porous microsphere packing as a medium for immobilizing anaerobic microorganisms, thereby facilitating biofilm formation. The flow state of the packing material at a high flow rate minimizes the risk of blockage and promotes efficient mixing between anaerobic microorganisms and wastewater, consequently enhancing treatment efficiency. Additionally, the reflux device incorporated in AFB facilitates substrate transfer and product outflow. The primary objective of this study is to enhance electricity generation performance in the Anammox AFB-MFC system and evaluate its nitrogen pollutant removal capability for high-nitrogen wastewater through laboratory experiments, providing a practical foundation for engineering applications. Additionally, we aim to characterize the physical properties of sludge aggregates within the reactor and analyze the microbial community composition using biological methods to further assess suitable operating conditions. Overall, this experiment conducted a 104-day performance testing period to gain comprehensive insights into the nitrogen removal and electricity generation performance of Anammox AFB-MFC.

2. Materials and Methods

2.1. Experimental Setup

The present study described the construction of a dual-chamber continuous flow Anammox AFB-MFC system, wherein both the anode and cathode chambers were fabricated using organic glass materials. The experimental setup is illustrated in Figure 2. Among them, the anode chamber was an AFB bioreactor equipped with a three-phase separator, and it had an effective volume of 10.66 L. The cathode chamber consisted of a reaction zone and a sedimentation zone. The reaction zone was designed as a columnar, low aspect ratio, fully mixed flow reactor, incorporating two baffles at each end to ensure optimal mixing efficiency. The effective volume of the reaction zone was 9.96 L, while the sedimentation zone had an effective volume of 3.81 L. The proton exchange membrane (DuPont, Nafilon-117, 20, Wilmington, DE, USA) was positioned between two polar chambers that were separated by a distance of 10 cm. Both the anode and cathode consisted of porous carbon paper (HCP030, 20 cm). A parallel arrangement was adopted for the placement of a 10 cm electrode with respect to the proton exchange membrane, maintaining a separation distance of 10 cm from the bottom.

The anode chamber of the reactor employed a reflux method to achieve a higher upward flow rate, thereby enhancing the stirring intensity and promoting thorough mixing of anaerobic bioparticles within the anode. Three microporous aeration heads are positioned at the base of the cathode chamber, where cathodic mixing is facilitated by an air compressor to establish an anaerobic environment. The aeration rate was regulated using a rotary flow meter. Copper wires connected the anode and cathode electrodes, while the operational output voltage was measured utilizing a UT70B professional electronic

multimeter. Additionally, during the reactor's start-up phase, a laboratory-prepared porous polymer material was introduced as a filler into the cathode chamber. The amount of filler added was 2 L, and it underwent screening through a 20–40 mesh sieve, exhibiting pronounced hydrophilicity and water absorption properties. It possessed low density, high fluidity, and provided an extensive surface area for microbial attachment.

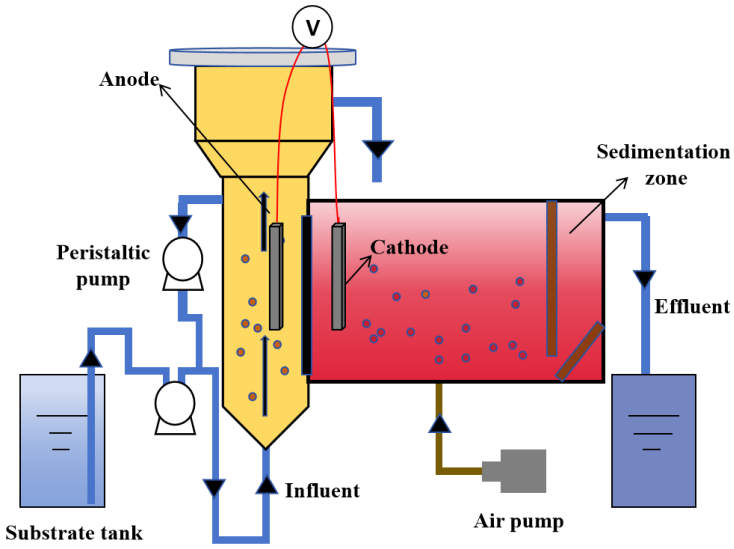

Figure 2. Operation conditions of the reactor.

The laboratory-prepared simulated wastewater was introduced into the anode chamber through a peristaltic pump located at the bottom. Following anaerobic treatment, it entered the cathode chamber from the top of the AFB. The effluent from anaerobic biological treatment in the cathode chamber flowed into the sedimentation zone and exited the reactor via a pump pipe connected to this zone. To ensure optimal activity of anaerobic microorganisms within both polar chambers, an electric heating wire wrapped around the exterior of the reactor was employed for temperature control, maintaining a constant temperature of 30 ± 3 °C. Furthermore, an opaque black covering is applied externally to the reactor in order to establish a light-restricted environment essential for the cultivation of anaerobic microorganisms.

The experiment was divided into two parts. To better investigate the impact of electricity generation on the reactor, it is crucial to establish an optimal operating environment for the system. In actual wastewater, organic matter inevitably exists, and when organic matter is present, substrate competition occurs between DNB and AnAOB sludge. A high concentration of carbon sources in wastewater significantly inhibits the growth and reproduction of AnAOB. Previous research has demonstrated that Anammox bacteria activity is inhibited or completely suppressed when COD exceeds 300 mg·L^{-1} [19]. Therefore, when studying the nitrogen removal performance of Anammox–MFC, it becomes essential to consider the influence of COD on these cells' performance. However, limited research has been conducted on how organic matter affects Anammox–MFC performance.

In the initial section, we evaluated the influence of organic matter on the performance of Anammox AFB-MFC. We established three concentration gradients for influent COD and assessed the nitrogen effluent concentration and output voltage of Anammox AFB-MFC at each gradient to ascertain optimal operational conditions for the reactor. Throughout this process, we maintained the HRT at 12 h. According to the conclusion of the preliminary experiment (Figure S2), we ensured an influent NH_4^+-N concentration of 200 mg/L and an influent NO_2^--N concentration of 200 mg/L. We employed a flow meter to regulate DO concentrations ranging from 0.5 to 1.0 mg/L and divided the influent COD concentration into three gradients: 100 mg/L, 200 mg/L, and 300 mg/L (Table 1). The MFC system was operated under three different concentration gradients, and effluent concentrations of NH_4^+-N, NO_2^--N, NO_3^--N, TN, and COD in both the anode and cathode chambers

of the reactor were recorded every two days. Additionally, the system's output voltage and power were also monitored. Each stage lasted for approximately 20 days. In the second section, the influent COD concentration was adjusted to match the appropriate concentration obtained from the first section while keeping other conditions constant. The circuit connecting the MFC anode and cathode was disconnected to transition the reactor from a closed to an open state. Recurring measurements of pollutant concentrations in two chambers every other day are conducted to facilitate a comparative analysis of pollutant removal rates between open and closed circuits, while simultaneously investigating the impact of electrical current on the nitrogen removal performance of Anammox AFB-MFC (Table 2). Mixed liquid suspended solid (MLSS) and mixed liquid volatile suspended solid (MLVSS) of both the anode and cathode were measured once a week.

Table 1. The operating conditions of the reactor under different COD conditions.

Phase	Duration (d)	HRT (h)	NH_4^+-N_{in} (mg/L)	NO_2^--N_{in} (mg/L)	DO (mg/L)	COD (mg/L)
I	1~21	12	200	200	0.5~1.0	100
II	22~41	12	200	200	0.5~1.0	200
III	42~60	12	200	200	0.5~1.0	300

Table 2. Exploration of power generation performance of Anammox AFB-MFC.

Phase	Duration (d)	HRT (h)	NH_4^+-N_{in} (mg/L)	NO_2^--N_{in} (mg/L)	DO (mg/L)	COD (mg/L)	Circuit (Open/Closed)
I	1~30	12	200	200	0.5~1.0	200	closed
II	31~58	12	200	200	0.5~1.0	200	open

2.2. Influent Wastewater Composition

The influent of this experiment consisted of artificially synthesized simulated wastewater, wherein ammonium chloride and sodium nitrite served as nitrogen sources, anhydrous glucose served as the carbon source, and anhydrous potassium dihydrogen phosphate served as the phosphorus source. The N:P was consistently maintained at 20:1, while sodium bicarbonate was employed to adjust the pH value of the influent within a range of 7.5 to 8.0. Furthermore, trace elements were supplemented as a nutrient solution to fulfill the growth requirements of microorganisms (Table S1).

2.3. Inoculum Sludge

The sludge inoculated in the reactor was a mixture of sludge and water obtained from the aeration tank of a specific kitchen waste comprehensive utilization center, which contains a small population of AnAOB. The sludge exhibits a brick red coloration. A total volume of 5 L of this sludge was inoculated into both the anode and cathode chambers. Furthermore, the anode chamber initially contained a minor quantity of anaerobic bioparticles. Following approximately 300 days of initial operation, the sludge within the reactor demonstrated favorable conditions and exhibited robust pollutant removal capabilities. On day one of this experiment, the MLSS concentration and MLVSS concentration in the anode chamber were 17.43 g/L and 13.82 g/L, and the MLSS and MLVSS concentrations in the cathode chamber were 5.01 g/L and 2.82 g/L, respectively.

2.4. Analysis and Calculations

The inlet and outlet water of the experiment was collected and measured every two days. Ultra-pure water was utilized for testing, while the analysis methods employed for assessing water quality are determined based on established standards [20] (Table S2).

The nitrogen loading rate (NLR), nitrogen removal rate (NRR), and nitrogen removal efficiency (NRE) are determined by calculating the balance of nitrogen and applying stoichiometry, as described in Equations (1)–(5) [21]. The standard curve for testing nitrides in this experiment is shown in Figure S1.

The system's output voltage was measured using a multimeter, and the power density of the output was calculated based on the anode area. The PA of the MFC anode area is expressed in Equation (6).

$$(\mathrm{TN})_{\mathrm{out}}(\mathrm{mg/L}) = \left\{(\mathrm{NH_4^+} - \mathrm{N}) + (\mathrm{NO_2^-} - \mathrm{N}) + (\mathrm{NO_3^-} - \mathrm{N})\right\}_{\mathrm{out}} \quad (1)$$

$$(\Delta \mathrm{N})(\mathrm{mg/L}) = \{(\mathrm{NH_4^+} - \mathrm{N}) + (\mathrm{NO_2^-} - \mathrm{N}) + (\mathrm{NO_3^-} - \mathrm{N})\}_{\mathrm{in}} - (\mathrm{TN})_{\mathrm{out}} \quad (2)$$

$$\mathrm{NLR}(\mathrm{kgN/m^3/d}) = \left\{(\mathrm{NH_4^+} - \mathrm{N}) + (\mathrm{NO_2^-} - \mathrm{N})\right\}_{\mathrm{in}}/\mathrm{HRT} \quad (3)$$

$$\mathrm{NRE_{TN}}(\%) = 1 - (\Delta \mathrm{N})/\left\{(\mathrm{NH_4^+} - \mathrm{N}) + (\mathrm{NO_2^-} - \mathrm{N}) + (\mathrm{NO_3^-} - \mathrm{N})\right\}_{\mathrm{in}} \quad (4)$$

$$\mathrm{NRR}(\%) = [\Delta \mathrm{N}]/\mathrm{HRT} \quad (5)$$

$$\mathrm{PA} = \frac{\mathrm{V^2}}{\mathrm{R_{ex}A_{anode}}} \quad (6)$$

In Equation (6), V is the output voltage, Rex is the external resistance, and A is the anode area.

2.5. Sequencing Using the Macrogene Platform

2.5.1. Extraction of DNA from Environmental Samples

We extracted 10 mL aliquots from the upper, middle, and lower anode layers, as well as 10 mL from the cathode. Subsequently, we subjected the collected samples to centrifugation at a speed of 5000 rpm for a duration of 15 min. Prior to removing precipitated DNA, we ensured that the sample was stored in a controlled environment at −20 °C. After the extraction of genomic DNA, 1% agarose gel electrophoresis was employed for the detection of the extracted genetic material. We fragmented it into 350 bp using ultrasonic breaker machine.

2.5.2. Reconstructing a Physical Education Library

(1) Joint connection. (2) We utilized magnetic beads for the screening and removal of self-connected fragments of the connector. (3) We enriched library templates through PCR amplification. (4) The final library was obtained by employing magnetic beads to recover PCR products.

2.5.3. PCR Amplification and Sequencing

(1) One end of the library molecule was hybridized with the primer base, and following amplification, the template information was immobilized on the chip. (2) The other end of the molecule was randomly hybridized with another nearby primer fixed on the chip, forming a "bridge". (3) PCR amplification generated DNA clusters. (4) The linearized DNA amplicon was converted into a single strand. (5) Modified DNA polymerase and dNTPs labeled with four fluorescent tags were added to synthesize only one base per cycle. (6) The reaction plate surface was scanned using a laser to determine the nucleotide types aggregated in the initial round of reactions for each template sequence. (7) Chemical cleavage of both the "fluorescent group" and the "termination group" restored 3′ end viscosity, enabling further polymerization of the second nucleotide. (8) Fluorescence signal results from each round were collected to obtain the sequence of template DNA fragments.

2.5.4. The Process of Bioinformatics Analysis

The data analysis commenced with the original sequence of the offline machine, wherein the initial sequence was optimized through procedures such as splitting, quality cutting, and contamination removal. Subsequently, these optimized sequences were employed for splicing assembly and gene prediction, followed by the annotation and classification of acquired genes based on species and function, encompassing the NR, EggNOG, and KEGG databases.

The revelations of the microbial community through comprehensive analysis were performed using the online platform of Majorbio Cloud Platform (www.majorbio.com, accessed on 2 February 2024).

3. Results and Discussion

3.1. The Impact of COD on Nitrogen Removal and Energy Production

According to the varying concentrations of COD in the influent, this experiment was divided into three distinct stages. The relevant nitrogen data were meticulously recorded and subsequently analyzed to determine the optimal COD concentration for Anammox AFB-MFC (Figure 3), thereby assessing its nitrogen removal performance.

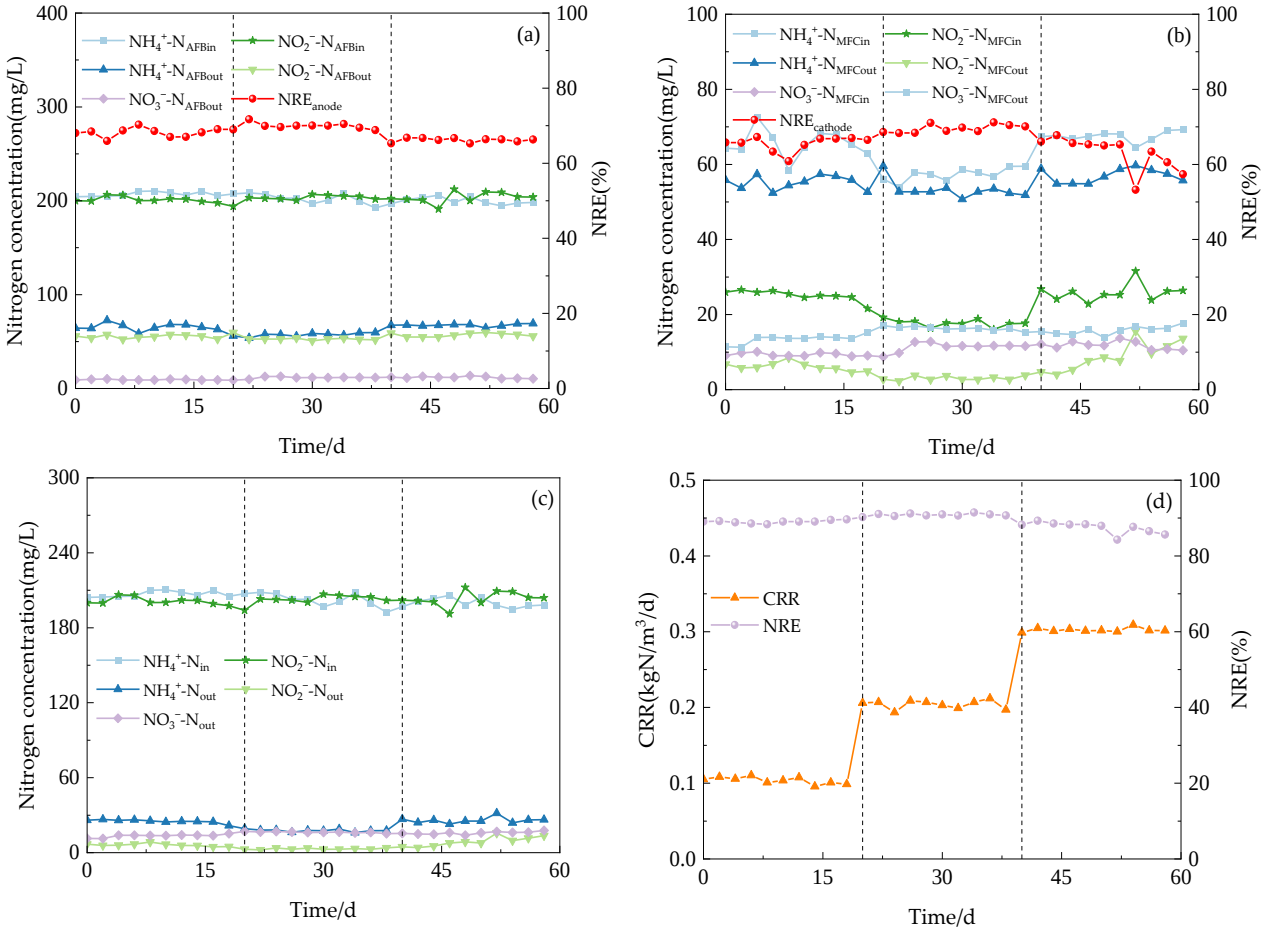

Figure 3. The performance of the reactor with continues operation. (**a**) Anodic nitrogen removal effect. (**b**) Cathode nitrogen removal effect. (**c**) Anammox AFB-MFC nitrogen removal effect. (**d**) COD load (CRR) and nitrogen removal efficiency (NRE).

The system exhibited a high capacity for the removal of both NH_4^+-N and NO_2^--N under three varying influent COD concentration gradients. During phase I (1–21 d), with an influent NH_4^+-N concentration of 209.98 mg/L, the effluent concentration at the anode for NH_4^+-N decreased to 58.48 mg/L, while at the cathode, it was measured as 25.10 mg/L. Simultaneously, with an influent NO_2^--N concentration of 200.13 mg/L, the effluent concentration at the anode for NO_2^--N reduced to 54.40 mg/L, and at the cathode, it reached a level of 8.51 mg/L. Anammox AFB-MFC also achieved lower nitrogen effluent concentrations in the other two stages, although there were slight differences in the NRE of the three stages (Figure 4a). At an influent COD concentration of 100 mg/L, the average NRE of the anode was 68.13%, while that of the cathode stood at 65.56%. Moreover, the overall average NRE reached 89.04%. During phase II (22–41 d), at an

influent COD concentration of 200 mg/L, the average NRE of the anode was 69.90%, the average NRE of the cathode was 69.58%, and the average NRE of the reactor was 90.85%. Increasing the influent COD concentration to 300 mg/L resulted in an average NRE of 66.18% for the anode; the average NRE of the cathode was 62.98%; and the average NRE of the reactor was 87.48%. Therefore, for optimal performance of the Anammox AFB-MFC system, it is recommended to maintain a consistent influent COD concentration at around 200 mg/L. The same conclusion can be inferred from the observation of the cathode NRE and the coupling system NRE: when the influent COD concentration was 200 mg/L, the reactor exhibited the highest NRE, indicating its strongest removal capacity for NH_4^+-N and NO_2^--N. This finding aligned with previous research by Chamchoi et al. [19], who investigated Anammox-coupled nitrogen removal in an UASB reactor using aquaculture wastewater. They observed a decrease in the NH_4^+-N removal rate by AnAOB when COD concentration exceeded 200 mg/L.

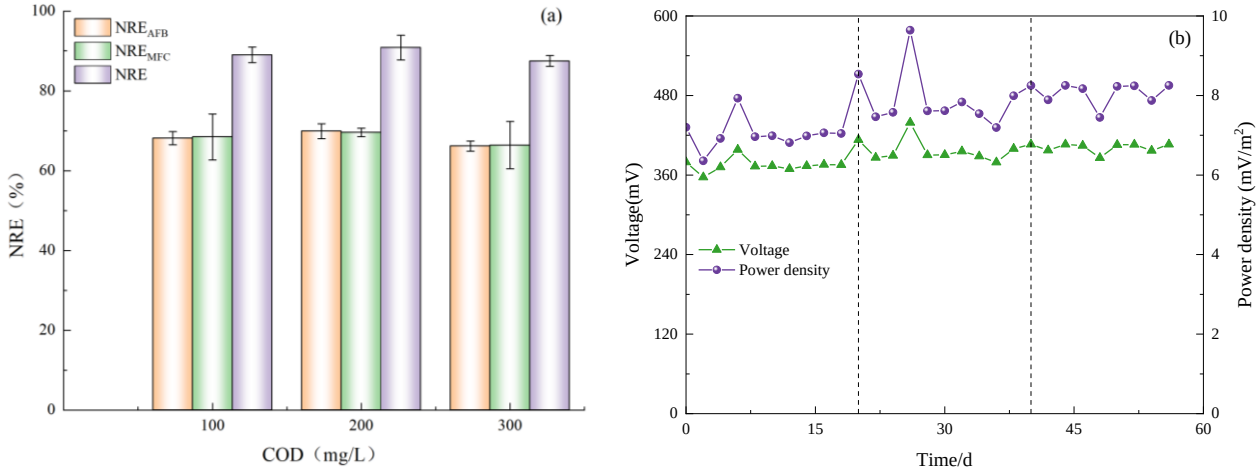

Figure 4. Nitrogen removal rate and electricity production performance. (**a**) NRE of anode (NRE_{AFB}); NRE of cathode (NRE_{MFC}); NRE of Anammox AFB-MFC (NRE). (**b**) Electricity generation performance of Anammox AFB-MFC.

In addition, a small amount of NO_3^--N was inevitably generated during the reaction process. According to the Anammox reaction mechanism, the production of NO_3^--N should account for 11% of the influent TN. However, in this experiment, when the influent TN concentration was approximately 400 mg/L, the observed production of NO_3^--N never exceeded 13 mg/L, significantly deviating from its theoretical value. This phenomenon can be attributed to the endogenous DNRA electron transfer mechanism exhibited by AnAOB bacteria. Specifically, AnAOB possesses the capability to sequentially convert NO_3^--N into NO_2^--N and NH_4^+-N through the enzymes Nar and NrfA [22]. Denitrifying bacteria can utilize intracellular carbon sources, such as polyhydroxyfatty acid esters (PHA) and glycogen, as electron donors to substitute external carbon sources in order to achieve NO_3^--N removal.

During this stage, the output voltage of the Anammox AFB-MFC exhibited fluctuations, characterized by significant decreases and increases (Figure 4b). It was hypothesized that variations in organic matter concentration may impact the power generation of the reactor, leading to a decline in the output voltage and power due to disruptions in the stable state of electricity-producing bacteria caused by changes in influent organic matter concentration. Gradually enriched methanogenic bacteria started competing with electricity-producing bacteria for organic substrates, resulting in reduced system power generation. Throughout this process, the output voltage ranged from a minimum of 356.6 mV to a maximum of 439.1 mV. In the final stage, MFC power generation tended to stabilize within a range of 380–410 mV. Hassan et al. [23] constructed an MFC reactor inoculated with AnAOB and employed the MFC anode for landfill leachate treatment. They observed that under high influent COD concentrations (800 mg/L), the power density of the MFC was

enhanced, which is consistent with our experimental findings. The average output voltage and power density of the MFC reached their peak values at the highest influent COD concentration. Furthermore, the formation process of bioparticles in the reactor is closely linked to electron and proton transfers at both the anode and cathode, potentially influencing voltage output performance, as influent substrate concentration and environmental conditions vary.

3.2. The Impact of Electricity Generation on Nitrogen Removal

The Anammox–MFC coupling system differs from traditional MFCs in its ability to generate voltage during nitrogen removal and beyond. While numerous studies have investigated the mechanisms of Anammox and MFCs for enhancing the nitrogen removal process, limited research has been conducted on the strengthening principle of nitrogen removal through the electric field generated by MFCs. Therefore, a comprehensive exploration of its working mechanisms is warranted.

The effect of system opening and closing on the nitrogen removal ability of Anammox AFB-MFC was investigated in this experiment. Figure 5 demonstrates that the MFC exhibited excellent removal efficiency for NH_4^+-N and NO_2^--N under both electricity-producing and non-electricity-producing conditions, owing to the efficient nitrogen removal ability of AnAOB. However, it can still be observed that electricity production has a certain impact on the system based on the nitrogen removal rates of the two stages under other identical conditions. During phase I, the average NRE of anode NH_4^+-N was 72.13%; the cathode NRE was 71.24%; and the reactor NRE was 91.62%. While in phase II, the NRE of the anode is 67.15%; the NRE of the cathode is 66.31%; and the NRE of the reactor is 88.93%. Notably, when operating in a closed-circuit state, Anammox AFB-MFC achieved an NRE exceeding 90%, which is significantly higher than that achieved in an open-circuit state. Similar conclusions were drawn from observing the removal efficiency for NO_2^--N and TN, indicating that the coupled system's nitrogen removal ability is stronger when operated in a closed-circuit state compared to an open-circuit state. This phenomenon may be attributed to enhanced activity of AnAOB due to electric field formation during closed-circuit operation, thereby improving overall nitrogen removal performance within the system. While electron accumulation may inhibit reaction progress under static open-circuit conditions, timely electron transfer occurs under closed-circuit conditions, promoting stable reaction progression [15].

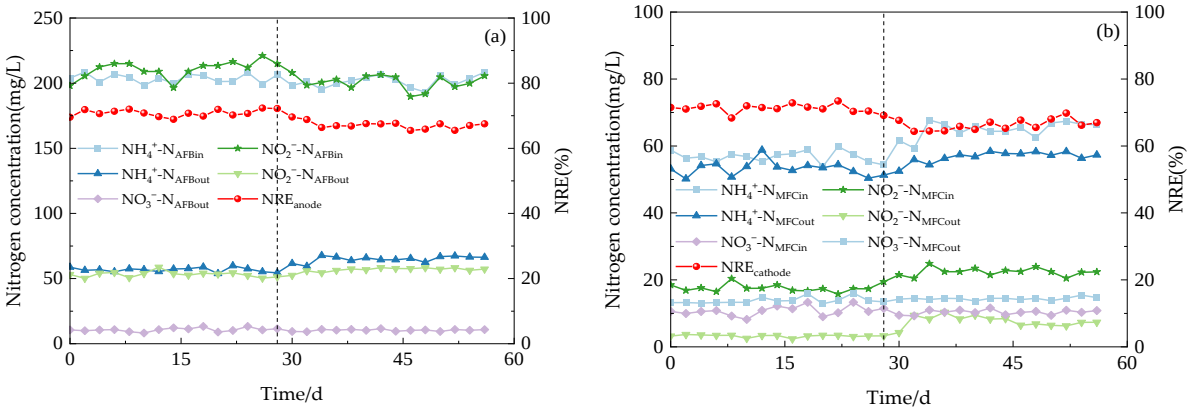

Figure 5. The performance of the reactor. (**a**) Anodic nitrogen removal effect. (**b**) Cathode nitrogen removal effect.

3.3. Change in Sludge Concentration and Bioparticle Analysis

With the continuous variations in experimental conditions, corresponding fluctuations in MLSS and MLVSS concentrations were observed within the anode and biological cathode regions of the system (Figure 6). By monitoring both concentration changes, it can be inferred that during the influent COD concentration alteration stage alone, both MLSS

and MLVSS exhibited an increasing trend. The initial MLSS value at the anode increased from 17.73 g/L to 23.65 g/L on 56 d, while the initial MLVSS value rose from 13.82 g/L to 19.16 g/L on day 56 as well. Similar upward trends were observed for the cathode region, with a gradual increase in the MLVS/MLSS ratio indicating enhanced microbial activity during this phase. This enhancement may be attributed to a progressive rise in influent organic matter concentration, which promoted microbial growth and metabolism within the cathodic chamber.

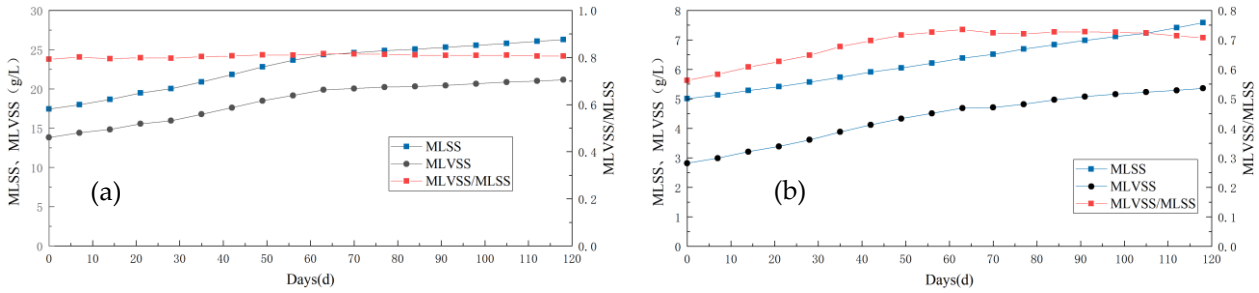

Figure 6. Variation in sludge concentration in the anode and cathode chamber of Anammox AFB-MFC. (**a**) MLSS and MLVSS in anode; (**b**) MLSS and MLVSS in cathode.

In both open- and closed-circuit experiments, the MLSS and MLVSS continued to improve, albeit at a significantly slower rate than in the previous stage. Upon examining their ratio, it was observed that the MLVSS/MLSS value was notably lower during the open-circuit phase compared to the closed-circuit phase, indicating a decrease in microbial activity within the reactor during this period—consistent with our earlier conclusion. During the open-circuit stage, deactivated black-brown bioparticles appeared in the outlet bucket of the reactor, whereas during its closed counterpart, water quality remained clear without any obvious bioparticles.

Due to the presence of heme in AnAOB cells, AnAOB appears red [24], and its bioparticles are also red [25]. Research has shown that AnAOB bioparticles exhibit excellent reaction performance [26], but their growth is greatly limited by substrate transfer. Anammox bioparticles cease to grow when they reach a certain particle size. As the influent substrate is consumed, cells inside the anaerobic bioparticles immediately become inactive and die. Some dead sludge is discharged from the reactor outlet, increasing the pollutant concentration in the effluent, while others become a new component of the bioparticles as nutrients enter the next life cycle of anaerobic bioparticles. Zhu et al. [27] found that Anammox bioparticles exhibited the highest activity when the particle size was between 0.5 and 0.9 mm. To improve the stability of Anammox and reduce the dissolution rate of bioparticle cells, fillers were added to the reactor for the attachment of anaerobic ammonia oxidation bacteria to fillers and the cultivation of anaerobic ammonia oxidation bioparticles.

In the initial stage, the liquid in both anode and cathode chambers appeared yellow-brown, while the mixture of mud and water in the cathode chamber had a lighter color. Upon the addition of Anammox sludge, initially both polar chambers retained their yellow-brown hue. However, with the continuous operation of the MFC coupling system, it was observed that the sludge gradually transitioned to orange-red and eventually turned reddish-brown, with particle sizes ranging from 1 to 5 mm. Simultaneously, there was a noticeable increase in the volume of bioparticles within the anode chamber. Due to the limited AFB volume, the bioparticles could not grow indefinitely; consequently, some bioparticles experienced cracking and loss of activity. Eventually, in the anode chamber, anaerobic bioparticles coexisted with flocculent sludge upon the cathode outlet discharge. Furthermore, slight discoloration was observed on the surface of a small amount of spherical packing in the cathode chamber, transitioning from white and light yellow to red. It is hypothesized that red AnAOBs on the packing's surface initiated growth. The MFC operation resulted in the transformation of some red particles into a black-brown color, accompanied by the peeling off of a layer of black film from the packing material. This

phenomenon is speculated to be attributed to the inactivation and cracking of AnAOB, with the detached film eventually being discharged through the cathode outlet. Figure 7a illustrates an image depicting the bioparticles within the reactor, while Figure 7b presents a visual representation of the bioparticles present in the reactor. It can be observed that these bioparticles formed within the MFC exhibit a spherical shape with predominantly orange-red coloration and particle sizes ranging from 1 to 3 mm.

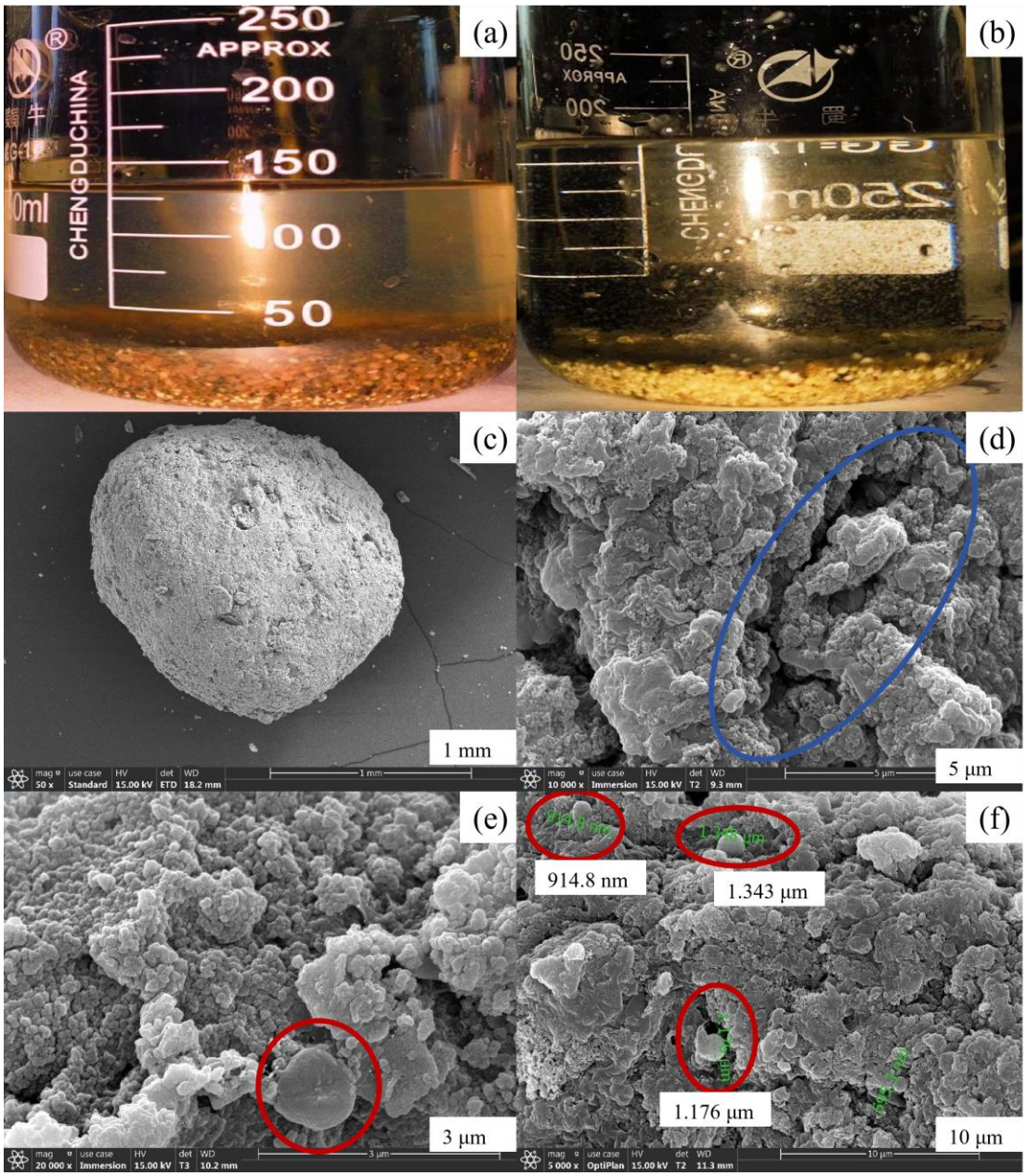

Figure 7. Variation in sludge concentration in the anode and cathode chamber of Anammox AFB-MFC. (**a**) Surface photos of bioparticles. (**b**) Superficial photos of bioparticles. (**c**) The overall morphology of bioparticles. (**d**) Rod-shaped bacteria on the surface of fillers. (**e**) Morphology of spherical bacteria on the surface of anode bioparticles. (**f**) Morphology of spherical bacteria on the surface of cathode bioparticles.

After undergoing dehydration treatment, the Anammox bioparticles were examined using scanning electron microscopy (SEM) to further investigate their microstructure.

The overall morphology of the anaerobic bioparticles is depicted in Figure 7c. From the figure, it can be observed that the particle size ranges between 1 and 3 mm, exhibiting a

spherical shape with some surface irregularities such as grooves, which facilitate microbial attachment (Figure 7d). The red circle in Figure 7e represents a spherical bacterium measuring approximately 1 µm in diameter, featuring a central depression that resembles a crater structure. This observation aligns with the previously reported morphology of AnAOB and thus suggests its potential identification as such. Furthermore, numerous spherical bacteria can be observed on the surface of bioparticles (Figure 7f), highlighted within the red circle, exhibiting diameters ranging from 0.9 to 1.4 µm, which is consistent with the defined size range for AnAOB. Therefore, these spherical bacteria are likely to be classified as AnAOB.

3.4. Microbial Community Analysis

In order to comprehensively investigate the evolutionary dynamics of microbial communities and account for the columnar architecture of AFB, a metagenomic analysis was conducted on bioparticle samples collected from the upper, middle, and lower regions of the anode AFB reactor, as well as sludge particles in the cathode chamber. Figure 8 illustrates the microbial composition and relative abundance at both the phylum and genus levels.

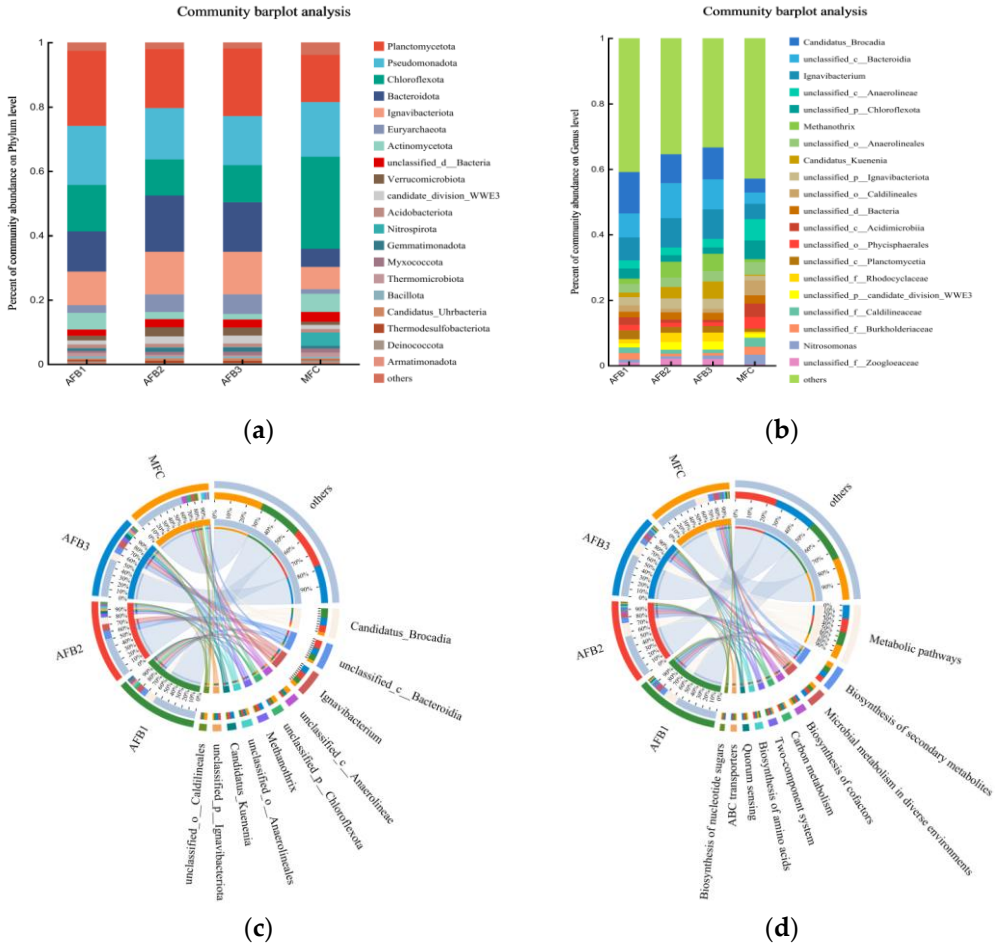

Figure 8. Anode bioparticles:AFB1 (lower), AFB2 (middle), AFB3 (upper), and MFC (cathode). (**a**) Microbial community distribution of Anammox AFB-MFC at phylum level; (**b**) microbial community distribution of Anammox AFB-MFC at genus level; (**c**) circos sample and species relationship diagram at genus level; (**d**) circos sample and function relationship diagram.

At the phylum level (Figure 8a), regarding the anode (bottom), the main bacterial communities in MFC sludge particles are *Planctomycota* (23.30%), *Pseudomonadota* (18.33%), *Chloroflexota* (14.48%), *Bacteroidota* (12.49%), and *Ignavibacteriota* (10.43%). The main bacterial communities in MFC cathode anaerobic sludge are *Chloroflexota* (28.60%), *Pseudomonadota* (16.99%), *Planctomycota* (14.66%), *Ignavibacteriota* (6.91%), and *Actinomycetota* (5.67%). The

research findings indicate that Anammox bioreactors harbor not only *Planctomycotes* but also *Proteobacteria*, *Bacteroidetes*, and *Chloroflexota*, aligning with the outcomes of this study [28,29]. In these advantageous communities, the current consensus recognizes AnAOB as a member of *Planctomycotes*, including *Candidatus Kunenia* and *Candidatus Brocadia*. The presence of a substantial population of AnAOB in MFC can be deduced in both anode and cathode. *Chloroflexota* is recognized as a pivotal microbial community in the degradation of carbohydrates [30]. It is also accountable for facilitating the maintenance of granular biofilms to a certain extent. *Ignavibacterota* is an anaerobic bacterium that is widely present in humid and hot environments. *Bacteroidota*, a microbial phylum closely associated with the formation of AnGS granulation, plays a crucial role in maintaining granulation through the secretion of EPS [31]. Furthermore, *Thermodesulfobacteriota* (0.69% in anode; 0.23% in cathode) exerts a predominant influence on the oxidation community of acetic acid substrates in bioelectrochemical systems and actively participates in bacteria's extracellular electron transfer process [32].

At the genus level (Figure 8b), the polar chambers harbor abundant and uniformly distributed microbial communities. The AnAOB bacteria dominated both electrode chambers of the MFC, constituting a significant proportion. *Candidatus Brocadia* exhibited an abundance of 12.62% in the lower layer of the anode, 8.84% in the middle layer, and 9.75% in the upper layer. *Candidatus Kunenia* demonstrated an abundance of 1.37%, 3.49%, and 5.29% in the respective layers of the anode. Regarding the cathode, *Candidatus Brocadia* exhibited an abundance of 4.23%, and *Candidatus Kunenia* accounted for 0.34%. The prevalence of these two types of AnAOB bacteria can be attributed to favorable and stable environmental conditions provided by the reactor. It can be observed that, irrespective of the anode or cathode chamber, *Candidatus Brocadia* exhibited significantly higher abundance in this reactor compared to *Candidatus Kunenia*, indicating a subtle complementary relationship. When the abundance of Candidatus Brocadia was high, the relative abundance of *Candidatus Kunenia* was low. Furthermore, the uneven distribution of these two types of AnAOB bacteria in AFB suggests that despite incorporating a reflux device, there still exists non-uniform mixing at the anode, resulting in selective enrichment of these bacteria at distinct positions. Research findings imply that at a low substrate concentration, *Candidatus Kuenenia* exhibits superior growth compared to *Candidatus Brocadia*. Conversely, at a high substrate concentration, *Candidatus Brocadia* demonstrates enhanced proliferation over *Candidatus Kuenenia* [33]. The nitrogen content in the wastewater prepared for this experiment is significantly elevated, resulting in a higher abundance of *Candidatus Brocadia*. Additionally, the cathode chamber exhibits a lower abundance of AnAOB bacteria compared to the anode chamber, potentially attributed to the continuous closure of the anode with minimal dissolved oxygen (DO) presence. Consequently, the anaerobic environment at the anode demonstrates enhanced stability. This finding further substantiates previous experimental outcomes and underscores that nitrogen removal capability is superior at the anode when contrasted with the cathode. In addition, *Thermomonas*, *Aquimonas*, *Thauera*, and *Simplicispira* also possess the capability to reduce nitrate [34]. *Hydrogenophaga* is recognized as a versatile denitrifying bacterium responsible for nitrate removal [35], and its enrichment confirms the occurrence of nitrogen removal in the reactor. *Nitrosomonas* and *Nitrospira*, representing AOB and NOB in bioparticles, respectively, play pivotal roles in driving nitrification reactions.

The activity of electricity-generating microorganisms directly determines the electricity production capacity of MFC. Previous experiments have demonstrated a positive correlation between MFC's electricity production capacity and system nitrogen removal, highlighting the significance of analyzing microorganisms associated with electricity generation in Anammox AFB-MFC for efficient nitrogen removal. *Paracoccus* (0.019%) is classified as a Gram-negative bacterium and exhibits diverse nitrogen metabolism pathways. It demonstrates the ability to utilize NO_3^--N, NO_2^--N, NO, and N_2O as substrates for metabolic processes. Furthermore, apart from nitrogen removal, *Paracoccus* has been acknowledged for its electrochemical activity. *Hydrogenophaga* (0.023%) is a Gram-negative bacterium capable of utilizing the byproducts of acetic acid metabolism in electrogenic bacteria. Consequently, *Hydrogenophaga* can establish a symbiotic relationship with electricity-producing bacteria, commonly coexisting with *Geobacter*

(0.033%), which are known for their ability to generate electrical current in MFC systems. *Ideonella* (0.014%) is classified as a Gram-negative bacterium and exhibits the ability to utilize various organic acids, amino acids, and carbohydrates as carbon sources. Moreover, this bacterium demonstrates anaerobic growth capabilities by employing chlorate as an electron acceptor. Notably, its strain, *Ideonelladechlorirans* sp., also possesses the capacity to utilize nitrate as a terminal electron acceptor [36]. *Klebsiella* (0.0039%) is a newly discovered electrochemically active bacterium [37], which has been identified as the dominant microbial community on the electrode surface in non-inoculated MFC electrochemical cathodes [38]. *Flavobacterium* (0.023%) is classified as a Gram-negative bacterium and has been detected in the majority of MFC. Previous literature has demonstrated its capacity for extracellular electron transfer [39]. *Acinetobacter* (0.032%) is classified as a Gram-negative bacterium and represents a prevalent electrogenic microorganism found in the cathode biofilm of MFC [40,41]. *Thauera* (0.027%) is a predominant bacterial genus in solid-phase nitrogen removal processes and also exhibits the ability to generate electricity through organic degradation in both aerobic and anaerobic MFC anodes [42]. This further enhances microbial aggregation, aerobic granulation, and partial nitrification–denitrification. Extensive research has demonstrated that *Pseudomonas* (0.092%) possesses the capability to generate a significant amount of electron shuttle mass, thereby significantly enhancing the power generation capacity of MFC [43]. *Shewanella*, commonly detected in MFC (0.0023%), were also observed in the reactor; however, their abundance was significantly diminished. The observed phenomenon could potentially be attributed to the prevailing anaerobic conditions within the reactor and the presence of Anammox bacteria specifically cultivated for nitrogen removal. Further investigation into this matter would yield valuable insights.

The distribution of species present in the four microbial samples is illustrated in Figure 8c, while Figure 8d displays the functional distribution within these samples. On the left side of both figures, the samples and their respective groups are depicted, whereas on the right side, the top ten dominant species are highlighted. The abundance distribution of different species across the samples is visualized through interconnected inner-colored bands.

In order to facilitate a more comprehensive comparison and analysis of the relationship between microbial communities in the anode and cathode chambers, we established a correlation network (Figure 9). The top 30 species were selected with the highest abundance for analysis. AnAOB was highlighted within a black box, with *Candidatus Brocadia* represented by a larger circle indicating higher abundance and *Candidatus Kunenia* represented by a smaller circle. In Figure 9, AnAOB exhibited a significant positive correlation with Planctomycetota and Ignavibacteriota while showing negative correlations with Pseudomonadota, Actinomycetota, Chloroflexota, and Nitrospirota. The coexistence of electricity-producing bacteria in Ignavibacteriota and AnAOB could potentially explain the synergistic effect between nitrogen removal and electricity production in the system. The presence of abundant AnAOB on the anode surface might inhibit the growth of other nitrogen-related bacteria, such as Actinomycetota with nitrogen-fixing ability. Additionally, Nitrospirota, as a typical NOB, displayed a negative correlation with AnAOB. Microbial correlation networks for both anode and cathode revealed that AnAOB was present in both polar chambers, particularly *Candidatus Brocadia* showed potential mutual promotion with electricity-producing bacteria but had a negative correlation with NOB.

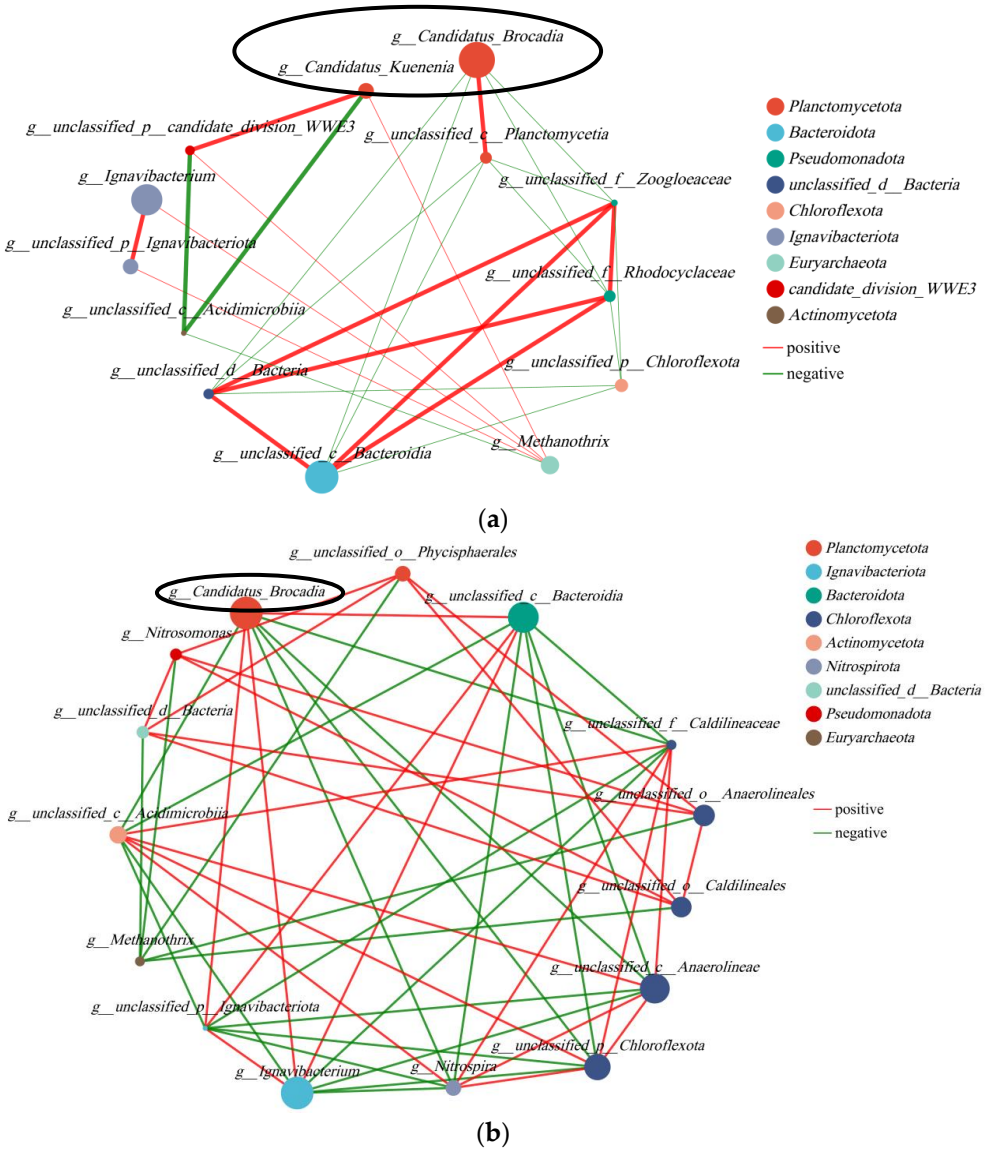

Figure 9. Correlation network: (**a**) analysis of anode; (**b**) analysis of cathode.

4. Conclusions

The Anammox AFB-MFC coupling system was operated in two stages. In the first stage, the reactor's influent COD concentration was explored to determine its suitability, while other conditions remained unchanged: NH_4^+-N and NO_2^--N were maintained at 200 mg/L, a constant temperature of 30 ± 3 °C was maintained, DO concentrations ranged between 0.5 and 1.0 mg/L, and HRT was set to 12 h. Three different concentration gradients of 100 mg/L, 200 mg/L, and 300 mg/L were tested. It was observed that the MFC exhibited the highest nitrogen removal efficiency when the influent COD concentration was set to 200 mg/L. In the second stage, the impact of electricity generation on MFC performance was investigated, and it revealed a positive effect on reactor nitrogen removal. In terms of the microbial community, *Candidatus Brocadia* and *Candidatus Kunenia* exhibited high abundance in both the anode and cathode chambers of the MFC. The overall abundance of *Candidatus Brocadia* surpassed that of *Candidatus Kunenia*, while various bacterial genera associated with electricity production, such as *Paracoccus*, *Hydrogenophaga*, and *Geobacter* had been identified in the bioparticles within the reactor. The enrichment or deactivation of rounded red bioparticles in the reactor may potentially influence nitrogen removal and electricity production performance, thereby impacting the overall functionality. Ultimately, under appropriate conditions, the reactor exhibited successful and stable nitrogen removal

as well as electricity generation capabilities, achieving an impressive NRE exceeding 90% alongside a remarkable electricity generation capacity surpassing 350 mV. The coexistence of AnAOB and electropositive microorganisms in the reactor synergistically enhances nitrogen removal efficiency and electricity generation in the system.

5. Discussion

Through a comparative analysis with previous studies on Anammox–MFC (Table S5), this experiment successfully achieved a high nitrogen removal rate within a shorter HRT. Consequently, it is recommended to increase the influent NH_4^+-N and NO_2^--N concentrations for domesticating AnAOB in order to effectively treat wastewater with higher nitrogen levels.

This experiment focuses on the nitrogen removal performance of the coupled system and investigates the impact of MFC's electricity generation performance on its nitrogen removal capacity. In subsequent experimental stages, further investigations will be conducted to explore MFC's electricity generation performance and circuit-related parameters in order to obtain more accurate optimal operating parameters, minimize MFC losses, and extend its lifespan.

Supplementary Materials: The following supporting information can be downloaded at https://www.mdpi.com/article/10.3390/su16072705/s1, Figure S1: Standard curve.; Figure S2: COD removal efficiency of the reactor.; Figure S3: Dynamics characteristics of NH_4^+-N reaction at different concentrations. Table S1: The trace element of nutrient solution; Table S2: Testing methods for various indicators; Table S3: Experimental instruments and equipment; Table S4: NH_4^+-N concentration and degradation rate. Table S5: The research progress of Anammox-MFC under different operating conditions. Refs [44–50] are cited in Supplementary Materials.

Author Contributions: Lead author, W.J.: Writing—Original Draft, Validation, Formal analysis, Visualization, Methodology, Data Curtion. Corresponding author, P.Y.: Writing—Review and Editing, Resources, Supervision, Project administration. Other authors, J.Z.: Resources, Validation. Q.Y.: Resources, Validation. All authors have read and agreed to the published version of the manuscript.

Funding: This research was funded by the Sichuan Development Environmental Science and Technology Research Institute Co., Ltd. (21H1038, 23H0010) and the Sichuan Provincial Industrial Wastewater Pollution Control and Low Carbon Resource Utilization Engineering Technology Research Center (2022YFQ0036).

Informed Consent Statement: Written informed consent has been obtained from the patient(s) to publish this paper.

Data Availability Statement: No new data were created or analyzed in this study. Data sharing is not applicable to this article.

Conflicts of Interest: Authors Wenqin Jiang, Ping Yang has received research grants from Sichuan Development Environmental Science and Technology Research Institute Co., Ltd. Authors Jian Zhang, Qiulin Yang were employed by the company Sichuan Development Environmental Science and Technology Research Institute Co., Ltd. The remaining authors declare that the research was conducted in the absence of any commercial or financial relationships that could be construed as a potential conflict of interest.

References

1. Ge, S.J.; Agbakpe, M.; Wu, Z.Y.; Kuang, L.Y.; Zhang, W.; Wang, X.Q. Influences of Surface Coating, UV Irradiation and Magnetic Field on the Algae Removal Using Magnetite Nanoparticles. *Environ. Sci. Technol.* **2015**, *49*, 1190–1196. [CrossRef]
2. Huang, J.Y.; Kankanamge, N.R.; Chow, C.; Welsh, D.T.; Li, T.L.; Teasdale, P.R. Removing ammonium from water and wastewater using cost-effective adsorbents: A review. *J. Environ. Sci.* **2018**, *63*, 174–197. [CrossRef] [PubMed]
3. Yu, C.Q.; Huang, X.; Chen, H.; Godfray, H.C.J.; Wright, J.S.; Hall, J.W.; Gong, P.; Ni, S.Q.; Qiao, S.C.; Huang, G.R.; et al. Managing nitrogen to restore water quality in China. *Nature* **2019**, *567*, 516–520. [CrossRef] [PubMed]
4. Zou, L.; Qiao, Y.; Li, C.M. Boosting Microbial Electrocatalytic Kinetics for High Power Density: Insights into Synthetic Biology and Advanced Nanoscience. *Electrochem. Energy Rev.* **2018**, *1*, 567–598. [CrossRef]
5. Kuenen, J.G. Anammox bacteria: From discovery to application. *Nat. Rev. Microbiol.* **2008**, *6*, 320–326. [CrossRef] [PubMed]

6. Zhang, Z.W.; Xu, C.Y.; Han, H.J.; Zheng, M.Q.; Shi, J.X.; Ma, W.C. Effect of low-intensity electric current field and iron anode on biological nitrate removal in wastewater with low COD to nitrogen ratio from coal pyrolysis. *Bioresour. Technol.* **2020**, *306*, 123123. [CrossRef] [PubMed]
7. Zhang, F.; He, Z. A cooperative microbial fuel cell system for waste treatment and energy recovery. *Environ. Technol.* **2013**, *34*, 1905–1913. [CrossRef] [PubMed]
8. Bian, B.; Shi, D.; Cai, X.B.; Hu, M.J.; Guo, Q.Q.; Zhang, C.H.; Wang, Q.; Sun, A.X.; Yang, J. 3D printed porous carbon anode for enhanced power generation in microbial fuel cell. *Nano Energy* **2018**, *44*, 174–180. [CrossRef]
9. Logan, B.E.; Hamelers, B.; Rozendal, R.A.; Schrorder, U.; Keller, J.; Freguia, S.; Aelterman, P.; Verstraete, W.; Rabaey, K. Microbial fuel cells: Methodology and technology. *Environ. Sci. Technol.* **2006**, *40*, 5181–5192. [CrossRef]
10. Do, M.H.; Ngo, H.H.; Guo, W.S.; Liu, Y.; Chang, S.W.; Nguyen, D.D.; Nghiem, L.D.; Ni, B.J. Challenges in the application of microbial fuel cells to wastewater treatment and energy production: A mini review. *Sci. Total Environ.* **2018**, *639*, 910–920. [CrossRef]
11. Pant, D.; Van Bogaert, G.; Diels, L.; Vanbroekhoven, K. A review of the substrates used in microbial fuel cells (MFCs) for sustainable energy production. *Bioresour. Technol.* **2010**, *101*, 1533–1543. [CrossRef] [PubMed]
12. He, Z.; Kan, J.J.; Wang, Y.B.; Huang, Y.L.; Mansfeld, F.; Nealson, K.H. Electricity Production Coupled to Ammonium in a Microbial Fuel Cell. *Environ. Sci. Technol.* **2009**, *43*, 3391–3397. [CrossRef] [PubMed]
13. Zhang, J.Q. *Simultaneous Nitrogen Removal and Electricity Generation in Microbial Fuel Cell and Its Mechanism*; Zhejiang University: Hangzhou, China, 2014.
14. Li, C.; Ren, H.Q.; Xu, M.; Cao, J.S. Study on anaerobic ammonium oxidation process coupled with denitrification microbial fuel cells (MFCs) and its microbial community analysis. *Bioresour. Technol.* **2015**, *175*, 545–552. [CrossRef] [PubMed]
15. Xu, M.Y.; Zhou, S.Q.; Liu, Z.J. Study on performance of dual-chamber MFC coupled with Anammox process in a high nitrogen load circumstancel. *Acta Sci. Circumstantiae* **2016**, *37*, 154–161. [CrossRef]
16. Song, C.K.; Wang, Y.Y.; Han, H.C. Effect of decreasing temperature on the performance and extracellular polymer substanceof anaerobic ammonia oxidation sludge. *China Environ. Sci.* **2016**, *36*, 2006–2013.
17. Yu, C.P.; Liang, Z.H.; Das, A.; Hu, Z.Q. Nitrogen removal from wastewater using membrane aerated microbial fuel cell techniques. *Water Res.* **2011**, *45*, 1157–1164. [CrossRef]
18. Chen, Z.H.; Huang, Y.; Li, X. Effect of PH on nitrogen conversion performance in the nitrification, ANAMMOX and combined process. *Environ. Eng.* **2016**, *34*, 55–60. [CrossRef]
19. Chamchoi, N.; Nitisoravut, S.; Schmidt, J.E. Inactivation of ANAMMOX communities under concurrent operation of anaerobic ammonium oxidation (ANAMMOX) and denitrification. *Bioresour. Technol.* **2008**, *99*, 3331–3336. [CrossRef]
20. The State Environmental Protection Administration; The Water and Wastewater Monitoring Analysis Method Editorial Board. *Water and Wastewater Monitoring and Analysis Methods*, 4th ed.; China Environmental Science Press: Beijing, China, 2002.
21. Vázquez-Padín, J.R.; Pozo, M.J.; Jarpa, M.; Figueroa, M.; Franco, A.; Mosquera-Corral, A.; Campos, J.L.; Méndez, R. Treatment of anaerobic sludge digester effluents by the CANON process in an air pulsing SBR. *J. Hazard. Mater.* **2009**, *166*, 336–341. [CrossRef]
22. Qiao, S.; Yin, X.; Zhou, J.T. Integrating anammox with autotrophic denitrification process by electrochemistry technology. *Chemosphere* **2018**, *195*, 817–824. [CrossRef]
23. Hassan, M.; Wei, H.W.; Qiu, H.J.; Su, Y.L.; Jaafry, S.W.H.; Zhan, L.; Xie, B. Power generation and pollutants removal from landfill leachate in microbial fuel cell: Variation and influence of anodic microbiomes. *Bioresour. Technol.* **2018**, *247*, 434–442. [CrossRef] [PubMed]
24. Kang, D.; Zheng, P.; Hu, Q.Y. Structure, morphology and function of Anammox granular sludge. *CIESC J.* **2016**, *67*, 4040–4046. (In Chinese)
25. Chen, H.; Ma, C.; Yang, G.F.; Wang, H.Z.; Yu, Z.M.; Jin, R.C. Floatation of flocculent and granular sludge in a high-loaded anammox reactor. *Bioresour. Technol.* **2014**, *169*, 409–415. [CrossRef] [PubMed]
26. Tang, C.J.; Duan, C.S.; Yu, C.; Song, Y.X.; Chai, L.Y.; Xiao, R.Y.; Wei, Z.S.; Min, X.B. Removal of nitrogen from wastewaters by anaerobic ammonium oxidation (ANAMMOX) using granules in upflow reactors. *Environ. Chem. Lett.* **2017**, *15*, 311–328. [CrossRef]
27. Zhu, G.B.; Wang, S.Y.; Ma, B.; Wang, X.X.; Zhou, J.M.; Zhao, S.Y.; Liu, R.P. Anammox granular sludge in low-ammonium sewage treatment: Not bigger size driving better performance. *Water Res.* **2018**, *142*, 147–158. [CrossRef] [PubMed]
28. Song, Y.X.; Liao, Q.; Yu, C.; Xiao, R.Y.; Tang, C.J.; Chai, L.Y.; Duan, C.S. Physicochemical and microbial properties of settled and floating anammox granules in upflow reactor. *Biochem. Eng. J.* **2017**, *123*, 75–85. [CrossRef]
29. Strous, M.; Pelletier, E.; Mangenot, S.; Rattei, T.; Lehner, A.; Taylor, M.W.; Horn, M.; Daims, H.; Bartol-Mavel, D.; Wincker, P.; et al. Deciphering the evolution and metabolism of an anammox bacterium from a community genome. *Nature* **2006**, *440*, 790–794. [CrossRef]
30. Miura, Y.; Watanabe, Y.; Okabe, S. Significance of *Chloroflexi* in performance of submerged membrane Bioreactors (MBR) treating municipal wastewater. *Environ. Sci. Technol.* **2007**, *41*, 7787–7794. [CrossRef]
31. Wei, Z.S.; He, Y.M.; Huang, Z.S.; Xiao, X.L.; Li, B.L.; Ming, S.; Cheng, X.L. Photocatalytic membrane combined with biodegradation for toluene oxidation. *Ecotoxicol. Environ. Saf.* **2019**, *184*, 109618. [CrossRef]

32. Zhu, K.L.; Wang, S.F.; Liu, H.; Liu, S.J.; Zhang, J.; Yuan, J.X.; Fu, W.C.; Dang, W.H.; Xu, Y.H.; Yang, X.; et al. Heteroatom-doped porous carbon nanoparticle-decorated carbon cloth (HPCN/CC) as efficient anode electrode for microbial fuel cells (MFCs). *J. Clean. Prod.* **2022**, *336*, 130374. [CrossRef]
33. Ding, S.; Zheng, P.; Lu, H.F.; Chen, J.W.; Mahmood, Q.; Abbas, G. Ecological characteristics of anaerobic ammonia oxidizing bacteria. *Appl. Microbiol. Biotechnol.* **2013**, *97*, 1841–1849. [CrossRef]
34. Han, F.; Wei, D.; Ngo, H.H.; Guo, W.S.; Xu, W.Y.; Du, B.; Wei, Q. Performance, microbial community and fluorescent characteristic of microbial products in a solid-phase denitrification biofilm reactor for WWTP effluent treatment. *J. Environ. Manag.* **2018**, *227*, 375–385. [CrossRef] [PubMed]
35. Zhang, B.; Li, W.; Wu, L.; Shi, W.X.; Lens, P.N.L. Rapid start-up of photo-granule process in a photo-sequencing batch reactor under low aeration conditions: Effect of inoculum AGS size. *Sci. Total Environ.* **2022**, *820*, 153204. [CrossRef] [PubMed]
36. Malmqvist, A.; Welander, T.; Moore, E.; Ternstrom, A.; Molin, G.; Stenstrom, I.M. Ideonella-dechloratans gen-nov, sp-nov, a new bacterium capable of growing anaerobically with chlorate as an electron-acceptor. *Syst. Appl. Microbiol.* **1994**, *17*, 58–64. [CrossRef]
37. Kim, G.T.; Webster, G.; Wimpenny, J.W.T.; Kim, B.H.; Kim, H.J.; Weightman, A.J. Bacterial community structure, compartmentalization and activity in a microbial fuel cell. *J. Appl. Microbiol.* **2006**, *101*, 698–710. [CrossRef] [PubMed]
38. Chung, K.; Fujiki, I.; Okabe, S. Effect of formation of biofilms and chemical scale on the cathode electrode on the performance of a continuous two-chamber microbial fuel cell. *Bioresour. Technol.* **2011**, *102*, 355–360. [CrossRef]
39. Wang, Z.J.; Zheng, Y.; Xiao, Y.; Wu, S.; Wu, Y.C.; Yang, Z.H.; Zhao, F. Analysis of oxygen reduction and microbial community of air-diffusion biocathode in microbial fuel cells. *Bioresour. Technol.* **2013**, *144*, 74–79. [CrossRef]
40. Liu, H.; Logan, B.E. Electricity generation using an air-cathode single chamber microbial fuel cell in the presence and absence of a proton exchange membrane. *Environ. Sci. Technol.* **2004**, *38*, 4040–4046. [CrossRef]
41. Zhang, G.D.; Zhao, Q.L.; Jiao, Y.; Zhang, J.N.; Jiang, J.Q.; Ren, N.; Kim, B.H. Improved performance of microbial fuel cell using combination biocathode of graphite fiber brush and graphite granules. *J. Power Sources* **2011**, *196*, 6036–6041. [CrossRef]
42. Yang, N.; Zhan, G.Q.; Li, D.P.; Wang, X.; He, X.H.; Liu, H. Complete nitrogen removal and electricity production in *Thauera*-dominated air-cathode single chambered microbial fuel cell. *Chem. Eng. J.* **2019**, *356*, 506–515. [CrossRef]
43. Zuo, Y.; Xing, D.F.; Regan, J.M.; Logan, B.E. Isolation of the exoelectrogenic bacterium *Ochrobactrum anthropi* YZ-1 by using a U-tube microbial fuel cell. *Appl. Environ. Microbiol.* **2008**, *74*, 3130–3137. [CrossRef]
44. Wang, H.Y.; Lyu, W.L.; Hu, X.L.; Chen, L.; He, Q.L.; Zhang, W.; Song, J.Y.; Wu, J. Effects of current intensities on the performances and microbial communities in a combined bio-electrochemical and sulfur autotrophic denitrification (CBSAD) system. *Sci. Total Environ.* **2019**, *694*, 133775. [CrossRef] [PubMed]
45. Lee, Y.; Martin, L.; Grasel, P.; Tawfiq, K.; Chen, G. Power generation and nitrogen removal of landfill leachate using microbial fuel cell technology. *Environ. Technol.* **2013**, *34*, 2727–2736. [CrossRef] [PubMed]
46. Guo, Y.L.; Wei, X.; Zhang, S.H. Simultaneous removal of organics, sulfide and ammonium coupled with electricity generation in a loop microbial fuel cell system. *Bioresource Technol.* **2020**, *305*, 123082. [CrossRef] [PubMed]
47. Li, Y.; Xu, Z.H.; Cai, D.Y.; Holland, B.; Li, B.K. Self-sustained high-rate anammox: From biological to bioelectrochemical processes. *Environ. Sci.-Water Res. Technol.* **2016**, *2*, 1022–1031. [CrossRef]
48. Zekker, I.; Bhowmick, G.D.; Priks, H.; Nath, D.; Rikmann, E.; Jaagura, M.; Tenno, T.; Tämm, K.; Ghangrekar, M.M. ANAMMOX-denitrification biomass in microbial fuel cell to enhance the electricity generation and nitrogen removal efficiency. *Biodegradation* **2020**, *31*, 249–264. [CrossRef]
49. Kong, Z.Y.; Zhou, Y.H.; Fu, Z.M.; Zhang, Y.C.; Yan, R. Mechanism of stable power generation and nitrogen removal in the ANAMMOX-MFC treating low C/N wastewater. *Chemosphere* **2022**, *296*, 133937. [CrossRef]
50. Zhang, L.; Jiang, M.H.; Zhou, S.G. Conversion of nitrogen and carbon in enriched paddy soil by denitrification coupled with anammox in a bioelectrochemical system. *J. Environ. Sci.* **2022**, *111*, 197–207. [CrossRef]